Journal of Petroleum Exploration and Production Technology (2023) 13:1691–1701
https://doi.org/10.1007/s13202-023-01640-3

REVIEW PAPER-PRODUCTION ENGINEERING

Calculation method of equivalent permeability of dual-porosity media considering fractal characteristics and fracture stress sensitivity

Xiang Luo[1] · Youyou Cheng[2] · Chengqian Tan[2]

Received: 18 August 2022 / Accepted: 25 April 2023 / Published online: 5 May 2023

Abstract

In the petroleum industry, the accurate calculation of equivalent permeability of dual medium is very important for the estimation of reserves and the design of oil and gas production. At present, there are many methods to calculate the equivalent permeability of dual medium. These methods have their own advantages and disadvantages, and are suitable for different medium characteristics and physical problems, but they cannot calculate the equivalent permeability of dual medium under reservoir conditions. Thus, the emergence of fractal theory provides a theoretical basis for us to study the law of fluid transport in randomly distributed pores and fractures. Many scholars have deduced the analytical solution of the fractal model of double-porosity media, and the fractal dimension of the rock matrix and fracture network has been widely used in the permeability model of dual-porosity media. It has been proven that fracture permeability and pore matrix permeability considering fractal properties can be realistically applied. In this work, the fractal dimension of the rock matrix and fracture network aperture surface tortuosity are introduced to establish a dual-permeability calculation model considering the fracture closure effect. Taking the Yanchi Chang 8 area of the Ordos Basin as an example, comparing the results of the numerical simulation model and fractal model, the proposed two-porosity medium model considering the stress closure effect is more accurate. The sensitivity analysis of each parameter in the equivalent permeability model shows that considering the effect of stress closure reduced the fracture and pore aperture. The equivalent permeability is significantly influenced by the fracture inclination, the fractal dimension of the fracture aperture, and the fractal dimension of the matrix pore diameter. The rougher fracture surface and more tortuous capillary path forces particles to move longer distances, thereby reducing the permeability of the fracture network.

Keywords Fractal dimension · Stress closure effect · Fluid-solid coupling · Dual-porosity media · Equivalent permeability

List of symbols

A_f	The cross sectional area of all the capillaries in the fracture network, μm^2
A_m	The cross sectional area of the unit, μm^2
A_p	The total pore area of the unit, μm^2
d_E	Euclidean dimension, Dimensionless
D_f	Fractal dimension for the size distribution of the fracture aperture after σ_{eff} is applied, Dimensionless
D_P	Fractal dimension for the size distribution of the matrix aperture (dimensionless), Dimensionless
D_T	Fractal dimension for the tortuosity of the matrix aperture (dimensionless), Dimensionless
D_x	Fractal dimension for the tortuosity of the fracture aperture after σ_{eff} is applied (dimensionless), Dimensionless
E	Young's modulus, GPa
H_f	Fracture aperture, μm
k	Proportionality constant, Dimensionless
K_f	Permeability of the fracture network, μm^2
K_m	Permeability of the rock matrix, μm^2
K_t	Equivalent permeability of dual-porosity media, μm^2
k_x	Fluid−solid coupling coefficient, Dimensionless
L	The length of the characterizing unit, μm
L_f	The length of the fracture unit, μm
L_{fo}	The initial length of the fracture unit, μm
L_0	The initial length of the characterizing unit, μm
L_{tf}	Tortuous length of a fracture, μm

✉ Xiang Luo
luoxiangxsyu@163.com

[1] School of Petroleum Engineering, Xi'an Shiyou University, Xi'an 710065, China

[2] School of Earth Science and Engineering, Xi'an Shiyou University, Xi'an 710065, China

L_{tf0}	Tortuous length of a fracture after σ_{eff} is applied, μm
L_t	Tortuous length of a capillary, μm
N	Cumulative number of fractures or porosity matrix, Unit
N_t	The total number of pores in porous media, Unit
Q_f	The total flow rate in fracture network, m^3
Q_m	The total flow rate in porosity matrix, m^3
r	Porosity matrix radius, μm
r_f	Fracture radius, μm
r_{fmin}	Minimum fracture radius, μm
r_{fmax}	Maximum fracture radius, μm
r_{f0min}	Minimum closure fracture radius, μm
r_{f0max}	Maximum closure fracture radius, μm
r_{min}	Minimum porosity matrix radius, μm
r_{max}	Maximum porosity matrix radius, μm
Δp	Differential pressure, MPa
θ	Fracture plane dip concerning flow direction in the front plane, °
υ	Poisson's ratio, Dimensionless
φ_m	Rock matrix porosity, Dimensionless
σ_{eff}	Effective stress on the fracture surface, m
σ_i	Normal stresses in the i direction, MPa
τ_{ij}/τ_{ji}	Shear stresses on the i and j planes, MPa
μ	Fluid viscosity, mPa s
ε	The strain vector of the rock skeleton, m

Introduction

The fracture shape in real reservoirs varies; that is, the distribution, length, orientation, and capillary radius of a fracture network in nature are usually disordered, there are few methods to find its analytical solution, and it is difficult to accurately characterize it in a dual-porosity media seepage model (Yu et al. 2017; Liu et al. 2018a, b; Zheng and Yu 2012; Li et al. 2016; Wei and Xia 2017; Berkowitz et al. 2022). Therefore, a large number of researchers believe that fractal geometry is an effective method to describe dual-porosity media (Lei et al. 2019; Xu et al. 2016; Luo et al. 2021; Sun et al. 2015). In addition, whether it is an artificial pressure fracture or natural fracture, under the action of the original stress, the fracture surface will reveal a closed state or tendency (Ghanbarian 2021; Jiang et al. 2013; Zhu and Cheng 2018; Zhang et al. 2021). With the continuous reduction in the pressure of the oil and gas reservoir, the effective closure stress of the fracture surface will also increase. Therefore, it is particularly important to calculate the equivalent permeability of fractures under different stress states (Cai et al. 2017; Xia et al. 2021, 2019; Mandelbrot 2006; Sarkheil et al. 2012).

Meanwhile, the spontaneous imbibition model in porous media and the model of unidirectional flow and multiphase flow in porous media with capillary forces have been solved by researchers (Sanei et al. 2015; Rigby et al. 2004; Xu et al. 2012). Later, Yu et al. (2003) proposed a new method of fractal-Monte Carlo simulation and then used this method to study the permeability of porous media. However, the spherical seepage in porous media is also significant (Yu et al. 2003; Hassani et al. 2011; Sarkheil et al. 2013a, b); thus, the spherical flow in porous media is implied by employing fractal theory, and the fractal solution of two-phase flow considering capillary force is obtained by Miao et al. (2018).

Most unconventional reservoirs have dual-media seepage problems. Therefore, many scholars have used fractal theory to describe the fracture network and pore structure of the porosity matrix and constructed expressions for the equivalent permeability of dual media (Chen et al. 2012; Miao et al. 2018; Liu et al. 2018a, b; Sarkheil et al. 2013a, b; Sarkheil et al. 2009). Chiles and Marisly (1993) proposed the relationship between the linear density, surface density, and volume density of fractures. Berkowiz and Hada (1997) believe that both natural and synthetic fracture networks have fractal characteristics, in which fracture surface density and fractal dimension are closely related. Meng et al. (2011) found that the surface density of fractures is positively correlated with the fractal dimension of fractures, and the surface density and fractal dimension of fractures jointly determine the development degree of fractures. Jafari and Babadagli (2011) obtained the fractal permeability expression of random fractures by multiple regression analysis based on logging observation data, which contained many empirical constants.

However, these expressions did not include the microstructure parameters of fracture tortuosity. Miao et al. (2015) obtained only the fractal permeability expression, including the tortuosity of the porosity matrix, according to the basic fractal theory of dual-porosity media. Therefore, to describe the pore structure of dual-porosity media more accurately, the fractal dimension of the tortuosity of the capillary wall in the fracture network should be introduced.

Although there are many results on the influence of fracture parameters on permeability, there is a lack of research on the quantitative influence of the fracture tortuosity fractal dimension and fluid−solid coupling coefficient on permeability. In this work, based on fractal geometry theory and models, a fractal model of equivalent permeability considering the tortuosity of fractures and the porosity matrix is established. The equivalent permeability of fractured porous media is calculated through the equation of fluid−solid coupling between fractures and the porosity matrix. The accuracy of the proposed model is verified by comparing the flow rate obtained by the model prediction with the numerical

simulation results, and a sensitivity analysis of each parameter in the model is carried out.

Theories and methodologies

In this section, we focus on the derivation of permeability models of the porosity matrix and fracture network, considering the fracture closure effect and fractal dimension of fracture tortuosity. The basis for calculating the equivalent permeability of dual-porosity media is presented in the next section.

Fractal theory for a porosity matrix

Many researchers have reported the fractal theory of porous media, which assumes that the matrix porous medium is composed of a bundle of curved capillaries, and the cumulative number of capillary diameters greater than or equal to r in the porous medium satisfies the following fractal scaling law (Yu et al. 2003):

$$N(L \geq r) = \left(r_{\max}/r\right)^{D_p} \tag{1}$$

The total number of pores in porous media is:

$$N_{\mathrm{t}}\left(L \geq r_{\min}\right) = \left(r_{\max}/r_{\min}\right)^{D_p} \tag{2}$$

In general, the number of capillary tubes or pores in porous media is very large, so Eq. (1) can be regarded as a continuous and differentiable function. By differentiating both sides of Eq. (1), we can obtain:

$$-\mathrm{d}N = D_p r_{\max}^{D_p} r^{-(D_p+1)}\mathrm{d}r \tag{3}$$

The probability density function of the porosity size distribution can be obtained by dividing Eq. (3) by Eq. (2):

$$f(r) = D_p r_{\min}^{D_p} r^{-(D_p+1)} \tag{4}$$

The density function $f(r)$ satisfies the normalization condition:

$$\int_{r_{\min}}^{r_{\max}} f(r)\mathrm{d}r = 1 - \left(r_{\min}/r_{\max}\right)^{D_p} = 1 \tag{5}$$

If the above formula is true, the condition $r_{\min}/r_{\max} << 1$ is satisfied, and the fractal dimension and ratio $(r_{\min}/r_{\max})$ of the porosity of fractal porous media meet the following relation:

$$\phi_m = \left(r_{\min}/r_{\max}\right)^{d_{\mathrm{E}}-D_p} \tag{6}$$

where d_{E} is the Euclidean dimension, $d_{\mathrm{E}}=2$ in 2D space, and $d_{\mathrm{E}}=3$ in 3D space.

The tortuosity of a curved flow path in porous media is defined as $\tau = L_{\mathrm{t}}/L_0$. The trace of fluid flow in a matrix curved capillary tub is usually curved and has fractal characteristics. The capillary diameter and length satisfy the following fractal scaling law:

$$L_{\mathrm{t}}(r) = r^{1-D_{\mathrm{T}}} L_0^{D_{\mathrm{T}}} \tag{7}$$

The total pore area representing the cross section of the unit is:

$$A_{\mathrm{p}} = -\int_{r_{\max}}^{r_{\min}} \frac{\pi r^2}{4}\mathrm{d}N = \frac{\pi D_p r_{\max}^2 (1-\phi_{\mathrm{m}})}{4(2-D_P)} \tag{8}$$

The cross sectional area of the unit is:

$$A_m = \frac{A_{\mathrm{p}}}{\phi_{\mathrm{m}}} = \frac{\pi D_p r_{\max}^2}{4\left(2-D_p\right)}\frac{1-\phi_{\mathrm{m}}}{\phi_{\mathrm{m}}} \tag{9}$$

If the characterizing unit is assumed to be a cube and the length of the characterizing unit is $L_0 = \sqrt{A_m}$, according to Poiseuille's law, the flow rate in a single curved capillary (Luo et al. 2021) is:

$$q(r) = \frac{\pi}{128\mu}\frac{\Delta p}{L_t} r^4 \tag{10}$$

Substituting Eq. (7) into Eq. (10) and integrating between the minimum and maximum pore sizes of all capillary tubes on the whole element body, we can obtain:

$$Q_{\mathrm{m}} = \frac{\pi L_0^{1-D_{\mathrm{T}}}}{128\mu}\frac{\Delta p}{L_0}\frac{D_p}{3+D_{\mathrm{T}}-D_p} r_{\max}^{D_T+3}\left[1-\left(\frac{r_{\min}}{r_{\max}}\right)^{D_{\mathrm{T}}-D_p+3}\right] \tag{11}$$

Based on $r_{\min} << r_{\max}$, then

$$Q_{\mathrm{m}} = \frac{\pi L_0^{1-D_T}}{128\mu}\frac{\Delta p}{L_0}\frac{D_p}{3+D_{\mathrm{T}}-D_p} r_{\max}^{D_{\mathrm{T}}+3} \tag{12}$$

The permeability of the porosity matrix can be obtained from Darcy's law:

$$K_{\mathrm{m}} = \frac{L_0^{1-D_{\mathrm{T}}}}{32}\frac{\phi_m}{\left(1-\phi_m\right)}\frac{\left(2-D_p\right)}{3+D_{\mathrm{T}}-D_p} r_{\max}^{D_{\mathrm{T}}+1} \tag{13}$$

Fractal theory for a fracture network

Previous studies have shown that the fracture network can be analogized to countless capillary bundles that satisfy fractal

scaling. According to basic fractal theory (Liu et al. 2018a, b), its fractal power-law relation is:

$$N(\geq r_{\mathrm{f}}) \propto r_{\mathrm{f}}^{-D_{\mathrm{f}}}, r_{\mathrm{f\,min}} \leq r_{\mathrm{f}} \leq r_{\mathrm{f\,max}} \tag{14}$$

Due to the large number of fractures in the fracture network, by differentiating Eq. (14), the number of fractures in the fracture network with capillary radii between [r, $r+\mathrm{d}r$] can be obtained as:

$$-\mathrm{d}N(r_{\mathrm{f}}) = kD_{\mathrm{f}} r_{\mathrm{f}}^{-(D_{\mathrm{f}}+1)}\mathrm{d}r_{\mathrm{f}},\ -\mathrm{d}N(r_{\mathrm{f}}) > 0 \tag{15}$$

The fracture probability density formula is:

$$-\frac{\mathrm{d}N(r_{\mathrm{f}})}{N_{\mathrm{t}}} = \frac{k}{N} D_{\mathrm{f}} r_{\mathrm{f}}^{-(D_{\mathrm{f}}+1)}\mathrm{d}r_{\mathrm{f}} = f(r_{\mathrm{f}})\mathrm{d}r_{\mathrm{f}} \tag{16}$$

where N_{t} represents the total number of fractures, and the probability density of fractures is normalized as:

$$\frac{k}{N_{\mathrm{t}}}\left(r_{\mathrm{f\,min}}^{-D_{\mathrm{f}}} - r_{\mathrm{f\,max}}^{-D_{\mathrm{f}}}\right) = \frac{k}{N_{\mathrm{t}}}\frac{1}{r_{\mathrm{f\,min}}^{D_{\mathrm{f}}}}\left(1 - \left(\frac{r_{\mathrm{f\,min}}}{r_{\mathrm{f\,max}}}\right)^{D_{\mathrm{f}}}\right) = 1 \tag{17}$$

When $r_{f\mathrm{min}} << r_{\mathrm{fmax}}$, Eq. (17) can be expressed as:

$$k = N_{\mathrm{t}} r_{\mathrm{f\,min}}^{D_{\mathrm{f}}} \tag{18}$$

When $r_{\mathrm{fmin}}/r_{\mathrm{fmax}} \leq 10^{-2}$, natural fracture networks generally meet the following requirement.

$$f(r_{\mathrm{f}}) = D_{\mathrm{f}} r_{\mathrm{f\,min}}^{D_{\mathrm{f}}} r_{\mathrm{f}}^{-(D_{\mathrm{f}}+1)} \tag{19}$$

The total number of fractures in the fracture network is:

$$N_{\mathrm{t}}(r_{\mathrm{f}}) = \left(r_{\mathrm{f\,max}}/r_{\mathrm{f\,min}}\right)^{D_{\mathrm{f}}} \tag{20}$$

Substituting Eq. (20) into Eq. (18) yields the proportionality constant

$$k = r_{f\,\mathrm{max}}^{D_f} \tag{21}$$

Then, by substituting Eq. (21) into Eq. (15), the fractal power-law relation of the capillary radius of the fractal fracture can be obtained:

$$-\mathrm{d}N(r_{\mathrm{f}}) = D_{\mathrm{f}} r_{\mathrm{fmax}}^{D_{\mathrm{f}}} r_{\mathrm{f}}^{-(D_{\mathrm{f}}+1)}\mathrm{d}r_{\mathrm{f}} \tag{22}$$

Yu et al. (2003) proposed a fractal scaling relation for fluid flow through random and complex fracture networks

$$L_{\mathrm{tf}} = r_{\mathrm{f}}^{1-D_x} L_{\mathrm{f}}^{D_x} \tag{23}$$

The cross sectional area of all the capillaries in the fracture network (Luo et al. 2021) is:

$$\begin{aligned} A_{\mathrm{f}} &= \int_{r_{\mathrm{f\,min}}}^{r_{\mathrm{f\,max}}} \frac{\pi r^2}{4}\mathrm{d}N(r_f) \\ &= \frac{\pi}{4}\frac{D_{\mathrm{f}}}{2-D_{\mathrm{f}}}\left[1 - \left(\frac{r_{\mathrm{f\,min}}}{r_{\mathrm{f\,max}}}\right)^{1-D_{\mathrm{f}}}\right] r_{\mathrm{f\,max}} \end{aligned} \tag{24}$$

Based on $r_{\mathrm{min}} << r_{\mathrm{max}}$, then

$$A_{\mathrm{f}} = \frac{\pi}{4}\frac{D_{\mathrm{f}}}{2-D_{\mathrm{f}}} r_{\mathrm{f\,max}} \tag{25}$$

To accurately describe the change in degree of fracture opening during the development process, it is assumed that the bulge of the fracture surface will not rupture during the effect of closure stress. In this case, the capillary diameter considering closure stress can be written as:

$$r_f = \left(1 - \sigma_{eff}/E\right) r_{fo} \tag{26}$$

The streamline length increases with increasing effective stress, as obtained by Gere and Goodno (2012):

$$L_{\mathrm{f}} = \left(1 + \sigma_{\mathrm{eff}}\upsilon/E\right) L_{\mathrm{fo}} \tag{27}$$

The relationship between the velocity and the pressure gradient of a single capillary tube in the fracture can be obtained by the Navier−Stokes equation

$$q(r_{\mathrm{f}}) = \frac{\pi}{128\mu}\frac{\mathrm{d}p}{\mathrm{d}L_{\mathrm{tf}}} r_{\mathrm{f}}^4 \tag{28}$$

If the total flow rate of the fluid through a component fracture collection is needed, the flow rate of the fluid through a single fracture should be obtained first, and then the minimum radius to the maximum radius of the capillary in all fractures on the entire characteristic element cross section should be calculated.

$$\begin{aligned} Q_{\mathrm{f}} &= \int_{r_{\mathrm{f\,min}}}^{r_{\mathrm{f\,max}}} q(r_{\mathrm{f}})\mathrm{d}N(r_{\mathrm{f}}) \\ &= \frac{\pi \Delta p D_{\mathrm{f}} r_{\mathrm{fo\,max}}^{3+D_x}\left(1 - \sigma_{\mathrm{eff}}/E\right)^{3+D_x}}{128 L_{\mathrm{fo}}^{D_x}\mu\left(3 + D_x - D_{\mathrm{f}}\right)\left(1 + \sigma_{\mathrm{eff}}\upsilon/E\right)^{D_x}}\left[1 - \left(\frac{r_{\mathrm{f\,min}}}{r_{\mathrm{f\,max}}}\right)^{3+D_x-D_{\mathrm{f}}}\right] \end{aligned} \tag{29}$$

In the two-dimensional plane, $0 < D_{\mathrm{f}} < 2$, $(r_{\mathrm{min}}/r_{\mathrm{max}})^{3+D_x-D_{\mathrm{f}}} << 1$, and according to Darcy's law, the above equation can be simplified as:

$$K_{\mathrm{f}} = \frac{\pi D_{\mathrm{f}} r_{fo\,\mathrm{max}}^{3+D_x}\left(1 - \sigma_{\mathrm{eff}}/E\right)^{3+D_x}}{128 L_{\mathrm{fo}}^{D_x-1} A_{\mathrm{f}}\left(3 + D_x - D_{\mathrm{f}}\right)\left(1 + \sigma_{\mathrm{eff}}\upsilon/E\right)^{D_x}} \tag{30}$$

Substituting Eq. (25) into Eq. (30), and if the fracture plane dip concerning the flow direction is θ, Eq. (30) can be written as:

$$K_{\mathrm{f}}=\frac{r_{\mathrm{fo\,max}}^{2+D_x}\left(1-\sigma_{\mathrm{eff}}/E\right)^{2+D_x}\left(2-D_{\mathrm{f}}\right)(\cos\theta)^{D_x-1}}{32L_o^{D_x-1}\left(3+D_x-D_{\mathrm{f}}\right)\left(1+\sigma_{\mathrm{eff}}\upsilon/E\right)^{D_x}} \tag{31}$$

Equivalent permeability model of dual-porosity media based on fractal theory

According to the equivalent permeability of the porosity matrix and fracture network presented in the previous section, the flow rate expression of the porosity matrix and fracture network can be obtained as follows:

Porosity matrix:

$$Q_{\mathrm{m}}=\frac{\pi L_0^{1-D_{\mathrm{T}}}}{128\mu}\frac{\Delta p}{L_0}\frac{D_p}{3+D_{\mathrm{T}}-D_p}r_{\max}^{D_{\mathrm{T}}+3} \tag{32}$$

Fracture network:

$$Q_{\mathrm{f}}=\frac{\pi\Delta pD_{\mathrm{f}}r_{\mathrm{fo\,max}}^{3+D_x}\left(1-\sigma_{\mathrm{eff}}/E\right)^{3+D_x}(\cos\theta)^{D_x}}{128L_o^{D_x}\mu\left(3+D_x-D_{\mathrm{f}}\right)\left(1+\sigma_{\mathrm{eff}}\upsilon/E\right)^{D_x}} \tag{33}$$

The characteristic units of the fracture network are larger than those of the pore matrix and contain multiple matrix units. Assuming $A_{\mathrm{f}}=n\,A_m$, Eq. (9) and (26) can be obtained as follows:

$$\frac{\pi}{4}\frac{D_{\mathrm{f}}}{2-D_{\mathrm{f}}}r_{\mathrm{f\,max}}=n\cdot\frac{\pi D_{\mathrm{p}}r_{\max}^2}{4(2-D_{\mathrm{p}})}\frac{1-\phi_{\mathrm{m}}}{\phi_{\mathrm{m}}} \tag{34}$$

Ignoring the interaction between the fluid in the pores of the porosity matrix and the fluid in the fracture network, the inflow and outflow of the fracture are equal, so the total flow rate of the medium with dual-porosity can be expressed as:

$$\begin{aligned}Q&=Q_{t,m}+Q_{\mathrm{f}}\\&=n\cdot\frac{\pi L_0^{1-D_{\mathrm{T}}}}{128\mu}\frac{\Delta p}{L_0}\frac{D_p}{3+D_{\mathrm{T}}-D_p}r_{\max}^{D_{\mathrm{T}}+3}\\&\quad+\frac{\pi\Delta pD_{\mathrm{f}}r_{\mathrm{fo\,max}}^{3+D_x}\left(1-\sigma_{\mathrm{eff}}/E\right)^{3+D_x}(\cos\theta)^{D_x}}{128L_o^{D_x}\mu\left(3+D_x-D_{\mathrm{f}}\right)\left(1+\sigma_{\mathrm{eff}}\upsilon/E\right)^{D_x}}\end{aligned} \tag{35}$$

where

$$Q_{t,m}=n\cdot Q_{\mathrm{m}} \tag{36}$$

The Newtonian fluid satisfies Darcy's law; then, the permeability expression of Newtonian fluid with dual porous media is:

$$\begin{aligned}K=&n\cdot\frac{L_0^{1-D_{\mathrm{T}}}}{32}\frac{\phi_{\mathrm{m}}}{\left(1-\phi_{\mathrm{m}}\right)}\frac{\left(2-D_p\right)}{3+D_{\mathrm{T}}-D_p}r_{\max}^{D_{\mathrm{T}}+1}\\&+\frac{r_{\mathrm{fo\,max}}^{2+D_x}\left(1-\sigma_{\mathrm{eff}}/E\right)^{2+D_x}\left(2-D_{\mathrm{f}}\right)(\cos\theta)^{D_x-1}}{32L_o^{D_x-1}\left(3+D_x-D_{\mathrm{f}}\right)\left(1+\sigma_{\mathrm{eff}}\upsilon/E\right)^{D_x}}\end{aligned} \tag{37}$$

However, when the fluid−solid coupling between the fracture network and porosity matrix is considered, the large error of the calculated permeability is compared with the actual permeability, resulting in an inaccurate reservoir description. Therefore, the permeability coupling factor is proposed to characterize the fluid−solid coupling between the fracture network and porosity matrix, as shown in Eq. (38):

$$K_t=K_{\mathrm{m}}+K_{\mathrm{f}}\cdot(1+k_x) \tag{38}$$

Then, the total permeability of the dual medium system is:

$$\begin{aligned}K_t=&\frac{L_0^{1-D_T}}{32}\frac{\phi_{\mathrm{m}}}{\left(1-\phi_{\mathrm{m}}\right)}\frac{\left(2-D_p\right)}{3+D_{\mathrm{T}}-D_p}r_{\max}^{D_{\mathrm{T}}+1}\\&+\frac{r_{\mathrm{fo\,max}}^{2+D_x}\left(1-\sigma_{\mathrm{eff}}/E\right)^{2+D_x}\left(2-D_f\right)(\cos\theta)^{D_x-1}}{32L_o^{D_x-1}\left(3+D_x-D_{\mathrm{f}}\right)\left(1+\sigma_{\mathrm{eff}}\upsilon/E\right)^{D_x}}\left(1+k_x\right)\end{aligned} \tag{39}$$

According to the lattice Boltzmann method, the equation of the permeability coupling factor is obtained by Yan (2019)

$$k_x=0.123\phi_{\mathrm{m}}^{0.838}H_{\mathrm{f}}^{-0.385\phi_{\mathrm{m}}^{0.285}} \tag{40}$$

Ultimately, the total permeability of the dual medium system is:

$$\begin{aligned}K_t=&\frac{L_0^{1-D_{\mathrm{T}}}}{32}\frac{\phi_{\mathrm{m}}}{\left(1-\phi_{\mathrm{m}}\right)}\frac{\left(2-D_p\right)}{3+D_{\mathrm{T}}-D_p}r_{\max^{D_{\mathrm{T}}+1}}\\&+\frac{r_{\mathrm{fo\,max}}^{2+D_x}\left(1-\sigma_{\mathrm{eff}}/E\right)^{2+D_x}\left(2-D_{\mathrm{f}}\right)(\cos\theta)^{D_x-1}}{32L_o^{D_x-1}\left(3+D_x-D_{\mathrm{f}}\right)\left(1+\sigma_{\mathrm{eff}}\upsilon/E\right)^{D_x}}\\&\left(1+0.123\phi_{\mathrm{m}}^{0.838}H_{\mathrm{f}}^{-0.385\phi_{\mathrm{m}}^{0.285}}\right)\end{aligned} \tag{41}$$

Table 1 List of calculation parameters

Parameter	Initial value	Range	Units	Parameter description
D_T	1.3	1.0 ~ 1.7	Dimensionless	Fractal dimension for the tortuosity of the matrix aperture
D_p	1.4	1.1 ~ 1.8	Dimensionless	Fractal dimension for the size distribution of the matrix aperture
D_x	2.3	1.0 ~ 2.7	Dimensionless	Fractal dimension for the tortuosity of the fracture aperture
D_f	1.5	1.1 ~ 1.8	Dimensionless	Fractal dimension for the size distribution of the fracture aperture
ϕ_m	11.0	10 ~ 45	%	Rock matrix porosity
L_0	150	–	μm	Length of the model
r	8	1 ~ 15	μm	Porosity matrix radius
r_f	15	1 ~ 35	μm	Fracture radius
H_f	35	–	μm	Fracture aperture
σ_{eff}	30	–	MPa	Effective stress on the fracture surface
υ	0.25	0.20 ~ 0.55	Dimensionless	Poisson's ratio of the fracture network
E	5.0	1 ~ 35	GPa	Young's modulus of the fracture network
θ	35	10 ~ 80	°	Inclination of the fracture direction relative to the horizontal direction

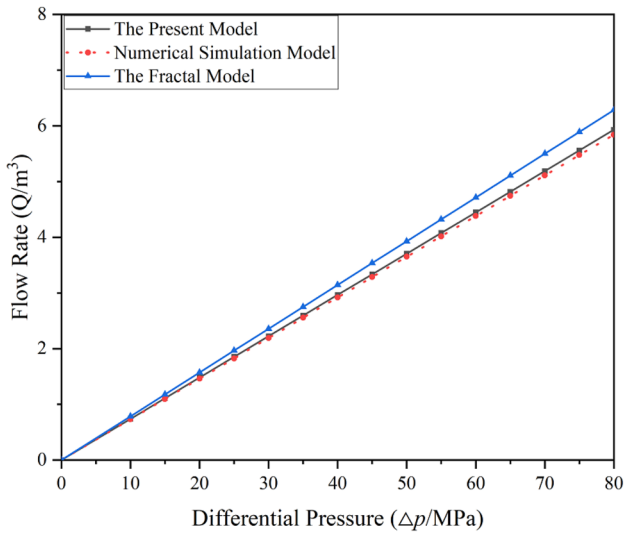

Fig. 1 Comparison of flow rate under different total permeability models

Results and discussion

Taking the Yanchi Chang 8 area of the Ordos Basin as an example, the equivalent permeability of double porous media is calculated. In this section, we use the Darcy seepage equation to calculate the flow rate. To verify the accuracy of the model, the model in this paper and the numerical simulation model were calculated. The parameters of the fractal model are shown in Table 1.

Figure 1 shows the predictions by the present model compared with those of the numerical simulation model and the fractal model. From Fig. 1, the fractal model predictions do not fit the numerical simulation results. In contrast, the present model predictions agree well with the numerical simulation data. Among them, the numerical simulation model is simulated by tNavigator, a commercial software developed by the Russian RFD company. Because the pore structure of rock satisfies the fractal geometry theory, the fractal model is Yu (Yu et al. 2003) numerical model proposed by A, which adopts the fractal distribution of pores. In this model, the porous medium is regarded as a space composed of fractal geometry.

By deriving the permeability equation of fractured reservoirs considering fracture closure, a series of flow rate charts were calculated and plotted to conduct sensitivity analysis. Below, the influence of fracture network parameters on flow rate is presented first, and then the effects of some key parameters on flow rate, including the fractal dimension of fracture tortuosity, maximum radius of the fracture network, and the physical parameters of the fracture network, are further discussed. For this case, consider fracture closure by Young's modulus (E), Poisson's ratio (ν), and effective stress (σ_{eff}) on a fracture network. Second, influence of the porosity matrix parameters on the flow rate is discussed, including the fractal dimension of the porosity matrix, fractal dimension of the porosity matrix tortuosity, maximum capillary radius, and matrix porosity.

Influence of fracture parameters on the flow rate of the permeability model

Figure 2 displays the effect of the fractal dimension of the fracture network and fracture tortuosity on the flow rate. The fractal dimension of the fracture and fracture tortuosity is negatively correlated with the flow rate. For a fixed fractal dimension of fracture tortuosity, a decrease in flow rate can be observed as the fractal dimension of the fracture increases. Meanwhile, the fractal dimension

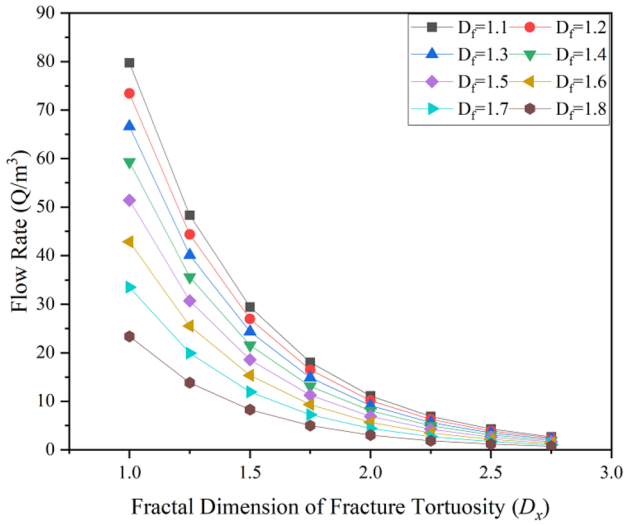

Fig. 2 Effect of the fractal dimension of the fracture network and fracture tortuosity on the flow rate

of fracture tortuosity has a larger impact on flow rate than the fractal dimension of fracture, and then the decreased range of flow rate decreases with the increase in the fractal dimension of fracture tortuosity and fracture. When the fractal dimension of the fracture tortuosity increased from 1.0 to 1.5, the flow rate decreased by 68.7%; when the fractal dimension of the fracture increased from 1.0 to 1.5, the flow rate decreased by 43.7%.

For a fixed fractal dimension of fracture, Fig. 3 shows the effect of the maximum fracture radius on the flow rate. It can be seen in Fig. 3 that the fracture radius has a significant effect on the flow rate. The fracture radius is

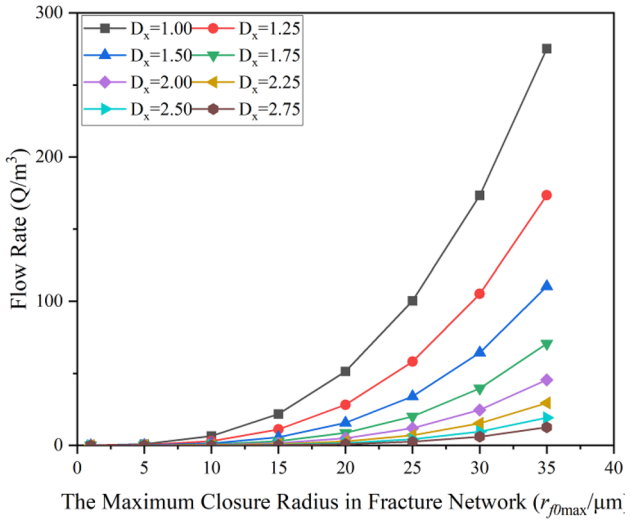

Fig. 3 Effect of the fractal dimension of fracture surface tortuosity and maximum fracture radius on the flow rate

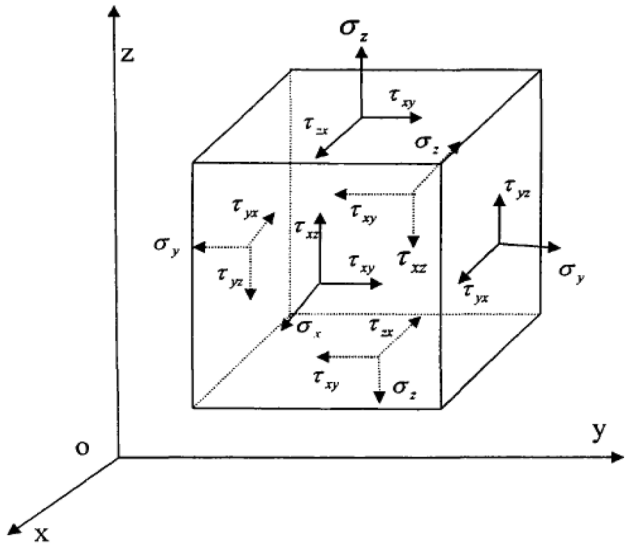

Fig. 4 Schematic diagram of forces acting on a rock element (Dai., 2006). Notes: σ_x, σ_y, σ_z are normal stresses in the x, y, and z directions; τ_{xy} and τ_{yx} are shear stresses on the x and y planes; τ_{xz} and τ_{zx} are shear stresses on the x and z planes; τ_{yz} and τ_{zy} are shear stresses on the y and z planes

positively correlated with the flow rate, and an increase in flow rate can be seen as the fracture radius increases.

Subsurface porous media rocks are composed of rock particles and pore fluids. During the development stage of the reservoir, compression of the rock will generate compound stress, which will lead to the deformation and displacement of the rock skeleton (Fig. 4). When the pore fluid migrates with the rock skeleton, relative seepage will also occur (Cao 2016; Wang et al. 2019).

As shown in Fig. 4, the reservoir rock can be equivalently regarded as a single hexahedral unit (Dai 2006; Feng et al. 2018). The opposite sides of the regular hexahedral elements are parallel to each other. Along the x, y, and z axes, the lengths of each side of the hexahedral unit correspond to dx, dy, and dz, respectively. The nine components on the reservoir rock are shown in Eq. (42). Moreover, the size of the nine components is related not only to the direction of the coordinate axis but also to the force of the point. The stress state at a certain point inside the rock can be represented in the form of a matrix:

$$\sigma_{ij} = \begin{bmatrix} \sigma_x & \tau_{xy} & \tau_{xz} \\ \tau_{yz} & \sigma_y & \tau_{yx} \\ \tau_{zx} & \tau_{zy} & \sigma_z \end{bmatrix} \tag{42}$$

Chen and Ewing (Chen and Ewing 1999) used the elastic physical equation of porous media to describe the relationship between the effective stress and strain of rock, and its general expression is:

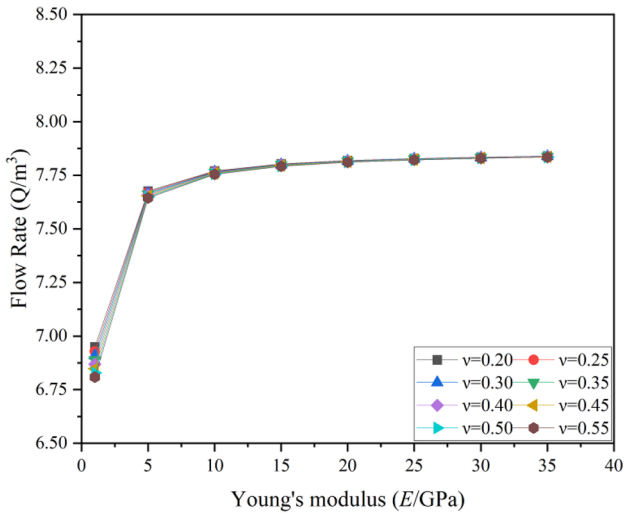

Fig. 5 Effect of Young's modulus (E) and Poisson's ratio (ν) of a fracture network on the flow rate

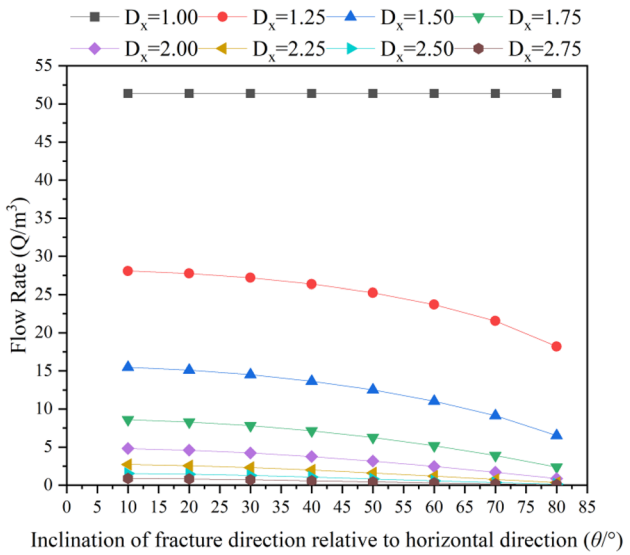

Fig. 6 Effect of the fractal dimension of the fracture surface tortuosity and inclination of the fracture direction relative to the horizontal direction

$$\{\sigma_{\text{eff}}\} = f(\{\varepsilon\}) \tag{43}$$

where $\{\sigma_{\text{eff}}\}$ is the stress vector of the rock skeleton, m; and $\{\varepsilon\}$ is the strain vector of the rock skeleton, m.

Meanwhile, as displayed in Fig. 5, Young's modulus has a significant influence on the flow rate. The flow rate increases significantly under the same Poisson's ratio, and when Young's modulus is between 1 and 10 GPa, the range of the flow rate change is relatively obvious. As shown in Fig. 5, the effect of Poisson's ratio on the flow rate is negligible.

Similarly, Fig. 6 shows that the flow rate gradually increases with increasing fracture inclination angle and slowly decreases in the initial stage, but with increasing fracture inclination angle in the later stage, the flow rate reduction rate is accelerated. According to the result analysis presented in Fig. 6, in this model, when the fractal dimension of the fracture network is 1, there is no correlation between the fracture inclination angle and flow rate.

Influence of porosity matrix parameters on the flow rate of the permeability model

Figure 7 displays the effect of the fractal dimension of the porosity matrix and porosity matrix tortuosity on the flow rate. The fractal dimension of the porosity matrix and porosity matrix tortuosity are negatively correlated with the flow rate. For a fixed fractal dimension of porosity matrix tortuosity, a decrease in flow rate can be observed as the fractal dimension of the porosity matrix increases. Meanwhile, the decreased range of the flow rate decreases with the increase in the fractal dimension of the porosity matrix tortuosity and porosity matrix. When the fractal dimension of the porosity matrix tortuosity increased from 1.0 to 1.5, the flow rate decreased by 0.9%; when the fractal dimension of the porosity matrix increased from 1.0 to 1.5, the flow rate decreased by 0.8%.

As shown in Figs. 8 and 9, the maximum porosity matrix radius and matrix porosity are positively correlated with the flow rate, but these two parameters have little impact on the flow rate.

Through comparison, we found that the fracture parameters have a significant influence on the porosity matrix parameters and the flow rate. In particular, the maximum

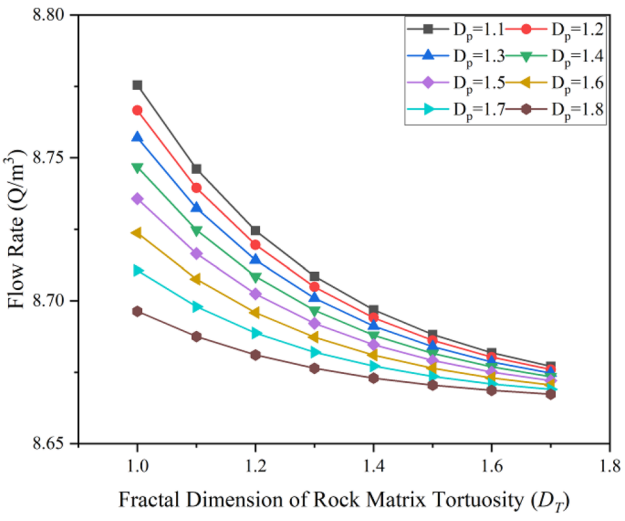

Fig. 7 Effect of the fractal dimension of the porosity matrix and porosity matrix tortuosity on the flow rate

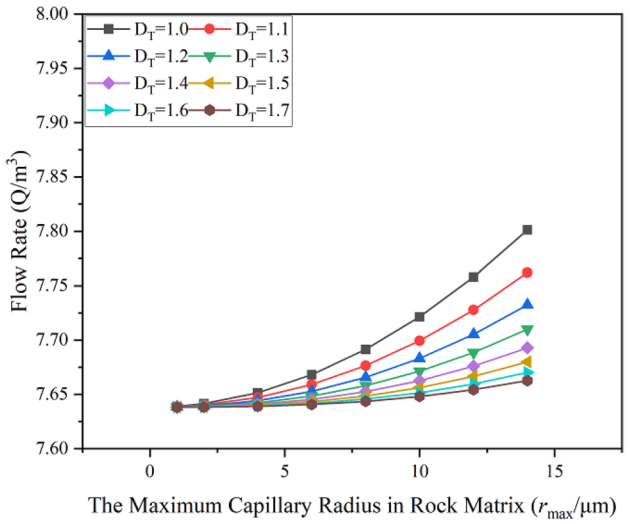

Fig. 8 Effect of the fractal dimension of porosity matrix surface tortuosity and the maximum capillary radius of rock matrix on the flow rate

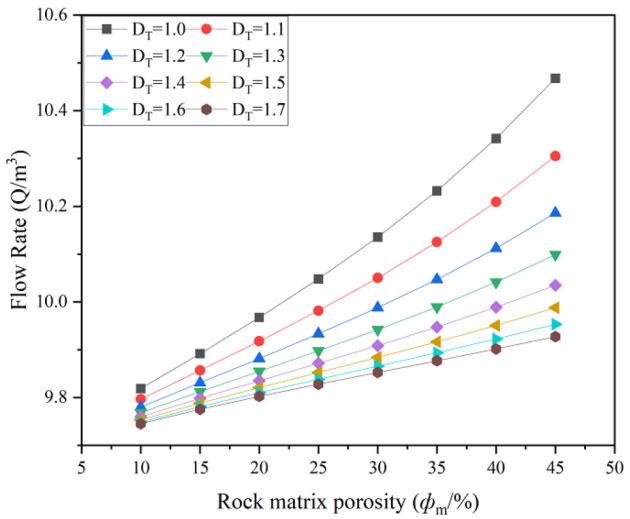

Fig. 9 Effect of the fractal dimension of the porosity matrix tortuosity and porosity matrix porosity on the flow rate

fracture radius, the fractal dimension of the fracture network, and fracture tortuosity have a significant influence on the flow rate, while the effect of the fractal dimension of the porosity matrix and porosity matrix tortuosity on the flow rate is weak. The difference between the fracture network and porosity matrix may demonstrate that the permeability of the fracture network is dominant in the equivalent permeability of dual-porosity media.

Conclusions

(1) The equivalent permeability of dual-porosity media can be described more accurately by considering the effect of stress closure and the fluid−solid coupling coefficient.
(2) The fractal dimension of the fracture diameter and tortuosity has a great effect on the equivalent permeability, and the fractal dimension of the fracture diameter and tortuosity is negatively correlated with the flow rate and equivalent permeability.
(3) The fracture closure effect has a weak influence on the flow rate, while the maximum fracture radius has a significant effect on the flow rate. With the increase in the fractal dimension of the fracture surface tortuosity, the rising trend of the flow rate slows with the increase in the maximum fracture radius.
(4) When the fracture inclination is less than 45°, it has a weak impact on the dual-porosity medium equivalent permeability; when the fracture inclination is greater than 45°, it has a significant impact on the dual-porosity medium equivalent permeability.
(5) With the increase in the fracture inclination angle, there is a significant decrease in the flow rate under the same fracture dimension of fracture surface tortuosity. When the fractal dimension of the fracture network is 1, there is no correlation between the fracture inclination angle and flow rate.
(6) The maximum matrix porosity radius and the matrix porosity are both positively correlated with the flow rate and equivalent permeability. The fractal dimensions of the matrix surface tortuosity and porosity matrix are both negatively correlated with the flow rate and equivalent permeability.

Acknowledgements We would like to express our deep gratitude to Shaanxi Provincial Department of Education and CNPC for providing the data used, support, and permission to get this paper published.

Funding The authors would like to acknowledge the support of the General Special Scientific Research Plan of the Shaanxi Provincial Department of Education (20JK0848) and the Scientific Research and Technology Development Project of CNPC (2021DJ3301).

Declarations

Conflict of interest We declare that we have no financial or personal relationships with other people or organizations that can inappropriately influence our work. There is no professional or other personal interest of any nature or kind in any product, service, and/or company that could be construed as influencing the position presented in the manuscript.

References

Berkowitz B, Hadad A (1997) Fractal and multifractal measures of natural and synthetic fracture networks. J Geophys Res 102(B6):12205–12218

Berkowitz B, Miller CT, Parlange MB, Hassanizadeh SM (2002) Characterizing flow and transport in fractured geological media: a review. Adv Water Resour 25(8–12):861–884

Cai JC, Wei W, Hu XY, Liu RC, Wang JJ (2017) Fractal characterization of dynamic fracture network extension in porous media. Fractals 25(02):1750023. https://doi.org/10.1142/S0218348X17500232

Cao HT (2016) Research on fracture surface morphology and seepage characteristics based on fractal theory, In: D. Chengdu University of Technology, pp 102–105

Chen Z, Ewing RE (1999) Mathematical analysis for reservoir models. SIAM Math Anal 30(2):431–453

Chen SJ, Zhu WC, Zhang MS, Yu QL (2012) Fractal description of rock joints based on digital image processing technique. Chin J Geotech Eng 34(11):2087–2092

Chiles JP, De Marsily G (1993) Stochastic models of fracture systems and their use in flow and transport modeling. Flow Contam Transp Fract Rock. pp 169–236

Dai P (2006) Experiment and numerical simulation of low permeability stress sensitive reservoir. Chengdu. Southwest Petroleum University, pp 70–73

Feng YL, Liu YT, Ding ZP (2018) Deformation characteristics and dynamic permeability model of a group of parallel fractures. Fault-Block Oil Gas Field 25(6):736–741. https://doi.org/10.6056/dkyqt201806010

Gere J, Goodno B (2012) Mechanics of materials. Cengage learning, Boston

Ghanbarian B (2021) Unsaturated hydraulic conductivity in dual-porosity soils: percolation theory. Soil Tillage Res 212:105061. https://doi.org/10.1016/j.still.2021.105061

Hassani H, Sarkheil H (2011) Fracture analysis in Tabnak hydrocarbon field of Iran by using fractal geometry and multi-fractal methods. In: European Geosciences Union, General Assembly, Austria

Jafari A, Babadagli T (2011) Effective fracture network permeability of geothermal reservoirs. Geothermics 40(1):25–38. https://doi.org/10.1016/j.geothermics.2010.10.003

Jiang GP, Shi W, Huang LL (2013) Fractal analysis of permeability of unsaturated fractured rock. Sci World J 5:490320. https://doi.org/10.1155/2013/490320

Lei G, Cao N, Mcpherson BJ, Liao QZ, Chen WQ (2019) A novel analytical model for pore volume compressibility of fractal porous media. Sci Rep 9:14472

Li B, Liu RC, Jiang YJ (2016) A multiple fractal model for estimating permeability of dual-porosity media. J Hydrol 540:659–669

Liu RC, Li B, Jiang YJ, Jiang HW, Yu LY (2018a) Relationship between equivalent permeability and fractal dimension of dual-porosity media subjected to fluid-rock reaction under triaxial stresses. Fractals 26(5):1850072. https://doi.org/10.1142/S0218348X1850072X

Liu R, Li B, Jiang YJ, Yu LY (2018b) A numerical approach for assessing effects of shear on equivalent permeability and nonlinear flow characteristics of 2-D fracture networks. Adv Water Resour 111:289–300

Luo YF, Xia BW, Li HL, Wu MY, Ji KN (2021) Fractal permeability model for dual-porosity media embedded with natural tortuous fractures. Fuel 295:120610. https://doi.org/10.1016/j.fuel.2021.120610

Mandelbrot B (2006) Fractal analysis and synthesis of fracture surface roughness and related forms of complexity and disorder. Int J Fract 138:13–17. https://doi.org/10.1007/s10704-006-0037-z

Meng QF, Hou GT, Pan WQ, Ju Y, Zhang QL, Li L, Shu WL (2011) Layer thickness controls on surface density and fractal dimension of structural fractures in carbonate strata. Geol J China Univ 17(03):462–468

Miao TJ, Yu BM, Duan Y, Fang QT (2015) A fractal analysis of permeability for fractured rocks. Int J Heat Mass Transf 81(81):75–80. https://doi.org/10.1016/j.ijheatmasstransfer.2014.10.010

Miao TJ, Chen AM, Xu Y, Zhang LW, Wang KD (2018) A permeability model for water-gas phase flow in fractal fracture networks. Fractals 26(6):1850087. https://doi.org/10.1142/S0218348X18500871

Rigby S, Wattsmith M, Fletcher R (2004) Simultaneous determination of the pore-length distribution and pore connectivity for porous catalyst supports using integrated nitrogen sorption and mercury porosimetry. J Catal 227(1):68–76. https://doi.org/10.1016/j.jcat.2004.06.025

Sanei M, Faramarzi L, Goli S, Fahimifar A, Rahmati A, Mehinrad A (2015) Development of a new equation for joint roughness coefficient (JRC) with fractal dimension: a case study of Bakhtiary dam site in Iran. Arab J Geosci 8:465–475. https://doi.org/10.1007/s12517-013-1147-3

Sarkheil H, Hassani H, Alinia F (2009) The fracture network modeling in naturally fractured reservoirs using artificial neural network based on image loges and core measurements. Aust J Basic Appl Sci 3(4):3297–3306

Sarkheil H, Hassani H, Alinia F, Enayati A, Nikandish A (2012) fracture analysis in Tabnak hydrocarbon field of Iran by using fractal geometry and multi-ractal analysis. Arab J Geosci 5(4):579–586. https://doi.org/10.1007/s12517-010-0214-2

Sarkheil H, Hassani H, Alinia F (2013b) Fractures distribution modeling using fractal and multi-fractal-neural network analysis in Tabnak hydrocarbon field, Fars Iran. Arab J Geosci 6(3):945–956. https://doi.org/10.1007/s12517-011-0400-x

Sarkheil H, Hassani H, Alinya F, Enayati AA, Motamedi H (2013a) A forecasting system of reservoir fractures based on artificial neural network and borehole images information-exemplified by reservoir fractures in Tabnak feild, fars, Iran, In: International Multidisciplinary Scientific GeoConference: SGEM: 1:563, 2013a, Surveying Geology & Mining Ecology Management (SGEM)

Sun W, Feng Y, Jiang C, Chu W (2015) Fractal characterization and methane adsorption features of coal particles taken from shallow and deep coalmine layers. Fuel 155:7–13

Wang L, Yang XY, Gong PZ, Zhang JT, Zhang B (2019) Study on stress sensitivity of middle-deep reservoirs in Bohai Sea: a case study of Kenli a oilfield. Petrol Geol Eng 35(03):50–54. https://doi.org/10.3969/j.issn.1673-8217.2021.03.010

Wei W, Xia Y (2017) Geometrical, fractal and hydraulic properties of fractured reservoirs: a mini-review. Adv Geo Energy Res 1(1):31–38

Xia Y, Cai J, Perfect E, Wei W, Zhang Q, Meng Q (2019) Fractal dimension, lacunarity and succolarity analyses on CT images of

reservoir rocks for permeability prediction. J Hydrol. https://doi.org/10.1016/j.jhydrol.2019.124198

Xia B, Luo Y, Pan C, Gong T, Hu H, Ji K (2021) Coalbed methane flow characteristics based on fractal geometry and stochastic rough fracture network. Energy Sour Part A 4:1–19. https://doi.org/10.1080/15567036.2020.1859015

Xu HF, Zhao PS, Li CF, Tong Q (2012) Predicting joint roughness coefficients using fractal dimension of rock joint profiles. AMM 170–173:443–448. https://doi.org/10.4028/www.scientific.net/AMM.170-173.443

Xu P, Li CH, Qiu SX (2016) A fractal network model for fractured porous media. Fractals 24(02):1650018. https://doi.org/10.1142/S0218348X16500183

Yan WC (2019) Research on seepage characteristics of formation based on digital core and digital wellbore, In: D. China University of petroleum (east China), pp 123–124

Yu BM, Li J, Li Z, Zou M (2003) Permeabilities of unsaturated fractal porous media. Int J Multiphase Flow 29(10):1625–1642. https://doi.org/10.1016/S0301-9322(03)00140-X

Yu L, Zhang L, Liu R, Jing H, Xie K (2017) Semi-empirical solutions for fractal-based hydraulic properties of 3D fracture networks. Géotech Lett 7(3):1–6

Zhang J, Wang YZ, Lou G, Kou JL (2021) A fractal model for effective thermal conductivity of dual-porosity media with randomly distributed tree-like networks. Fractals 29(06):2150146. https://doi.org/10.1142/S0218348X21501462

Zheng Q, Yu BM (2012) A fractal permeability model for gas flow through dual-porosity media. J Appl Phys 111(2):024316

Zhu JT, Cheng YY (2018) Effective permeability of fractal fracture rocks: Significance of turbulent flow and fractal scaling. Int J Heat Mass Transf 116:549–556. https://doi.org/10.1016/j.ijheatmasstransfer.2017.09.026